HONGMEI LIU
XIA MENG
WEI HE
and
RONG LI

Inversion of rheological parameters of surrounding rocks in a mine roadway based on BP neural network

For weak rock mass with notable rheological property, instability is mostly caused by flowing deformation. As the basis for the design of roadway supporting structure, the rheological parameters of surrounding rocks are of great importance. Unfortunately, the rheological parameters obtained from indoor tests often fail to reflect the geological defects in a large research area due to the impact from constraints of sampling representativeness, sampling disturbance and testing technical level. What is worse, field tests are time-consuming, unrepeatable and costly. To solve these problems, this paper conducts inversion of the rheological parameters of surrounding rocks based on the BP neural network. Taking a mine roadway as an example and considering the vault subsidence data in the entrance section, the author applies FLAC^{3D} in numerical simulation, adopts BP neural network for network learning and sample training, and performs displacement inversion of the rheological parameters of the surrounding rocks in the section.

Keywords: Numerical simulation; creep; BP neural network.

1. Introduction

The research on rock rheological property could be traced back to the 1930s. In 1939, Griggs [1] suggests that creep deformation takes place when the load reaches 12.5-80% of the failure load and employs the logarithm empirical equation to describe the constitutive relation of rock rheology on the basis of compression-creep tests on sandstones, argillite and siltstones. In 1991, Professor Chen Zongji [2] designs a torsional creep apparatus to perform torsional creep test on sandstones in Yichang and proposes a hypothesis regarding the origin and formation of the "enclosed" stress. Besides, the professor examines the release of internal strain energy, conducts 3D expansion to the test equations proposed by Griggs, and takes material parameters as the scalar functions of the stress invariant.

In 1991, Shi Yuchuan et al. [3] hold a field survey targeted at the weak rock belt of dam abutment on the right bank of Ertan hydropower station, build the H-K model, a rheological model suitable for the weak rock mass in the following indoor and field rheological tests, and determine the constitutive equation of the weak rock mass based on the curves from the field tests and the finite element inversion method. In 2000, Zhou Huoming et al. [4] from Changjiang River Scientific Research Institute of Changjiang Water Resources Commission perform compression-creep tests on the rock mass of the side slope of the permanent ship lock in the Three Gorges Dam Project, make comprehensive analysis of the creep test results on indoor soil mass and field rock mass, and put forward the method for determining the value of rock mass creep parameter through inversion of viscoelastic displacement.

Since the emergence of the artificial neural network, [5-9] the neural network, especially the back propagation neural network (BP neural network), has been effectively employed to solve non-linear problems and extensively applied in various fields. Being one of the most commonly used networks, BP neural network [10] is a multilayer feedforward network that minimizes the error sum of squares of the network by using gradient descent method and back propagation to adjust the weight and threshold of the network.

This paper, therefore, applies the BP neural network in inversion of rheological parameters of surrounding rocks. The application can effectively resolve the difficulties in undermining the rheological parameters resulted from testing conditions and external environment. Moreover, taking a mine roadway as example and considering the vault subsidence data in the entrance section, this paper applies FLAC^{3D} in numerical simulation, adopts BP neural network for network learning and sample training, and performs displacement inversion of the rheological parameters of the surrounding rocks in the section.

Messrs. Hongmei Liu and Rong Li, Department of Information Technology, Beijing Vocational College of Agriculture, Beijing 102 442, Xia Meng*, Architectural Design and Research Institute of Tsinghua University Co. Ltd., Beijing 100 084 and Wei He, Department of Civil Engineering, Tsinghua University, Beijing 100 084, China. Email: 240498175@qq.com

2. Establishment of the numerical calculation model for roadway excavation

The process of soft rock roadway excavation and support is undoubtedly related to the stress path because it is mainly about the loading and unloading surrounding rocks. In this sense, the reliability of inversion results hinges on the actual simulation of the excavation and supporting process. Hence, the author takes a mine roadway as example for modelling.

According to engineering geological mapping and drilling, the rock mass in the roadway area is formed in the Yanshanian period (r_5^3). In the exposure zone, the formation lithology is granodiorite (r_5^3), lying below the alluvial soil layer of the quaternary system. The surrounding rocks near the roadway section are severely-to-medially weathered granodiorite. The relatively hard rock has 3 groups of cracks distributed by volume gap rate $Jv=15$ pieces/m^3. There is trickling water at the entrance and exit of the roadway with the [BQ] value ranging from 251 to 350. The roadway is constructed by the three-bench method as a guarantee of construction safety and quality.

2.1 Boundaries of computational simulation

According to Saint-Venant's Principle, the influence from excavation on surrounding rocks gradually disappears as the excavation position moves farther away. The target area within the boundaries of computational simulation should be determined through comprehensive consideration of computational efficiency and accuracy. After thorough consideration of factors like the geology in the roadway region, the target of computational simulation is determined as the area within the following boundary lines: the left and right lines are 75m away from the center point of the grotto, the bottom line is 53m away from the point, the upper line is the terrain surface, and the direction of roadway excavation is 100m. In the model, the surrounding rocks and the first lining are simulated with hexahedron block units and cable bolt units. As shown in Fig.1, there are in total 347,400 units and 361,479 nodes.

The steel arch centering is subjected to the equivalent numerical simulation, that is, the effect of steel arch centering is converted to the effect of shotcrete. The goal is to improve the rigidity and elasticity modulus of the shotcrete. The roadway bolts are simulated with cable bolt units because the bolts are mainly characterized by axial strength. Figs.1, 2 and 3 respectively illustrate the side view of the computational model, the equivalent reinforced model of advanced small pipe, and the cable bolt units of the first lining.

2.2 Numerical simulation of the construction process

The roadway entrance is excavated by the three-bench seven-step method for construction, which drives in 1m at a time. Each bench is 5m-long and the core soil is 3m long. Construction steps are as follows (Fig.4):
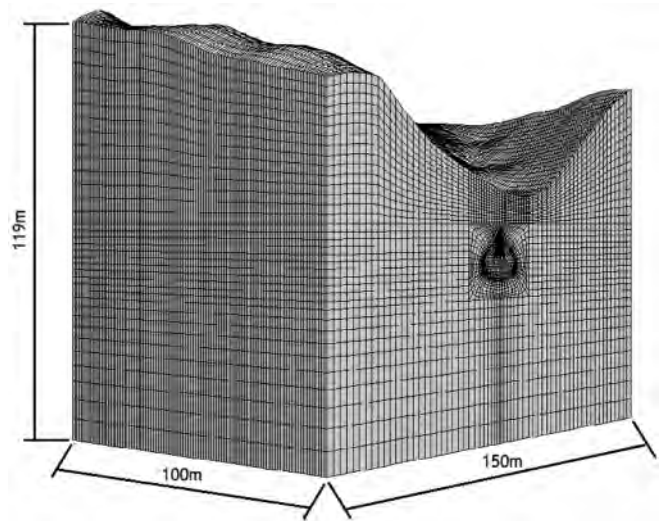

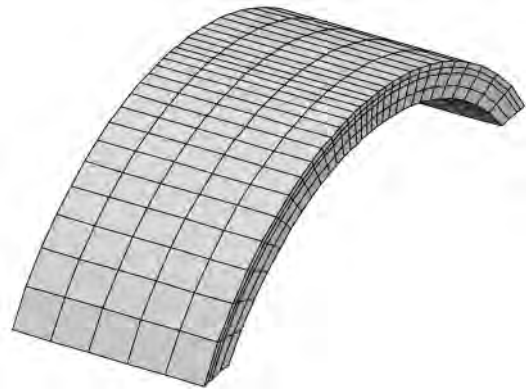Fig.1 Side view of the computational model

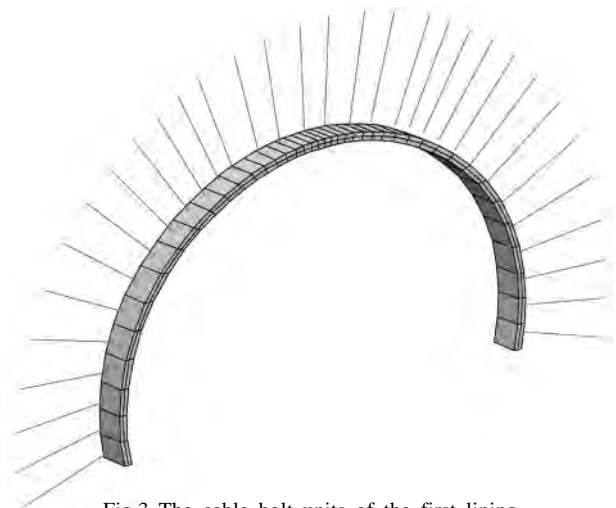Fig.2 Equivalent simulation model based on advanced small pipes

Fig.3 The cable bolt units of the first lining

The roadway is excavated in the following order: First, use the steel frame set up in the previous cycle to lay a single layer of advanced small pipes at a circumferential spacing of 0.4m within the 1a upper chamber, and inject slurry with water
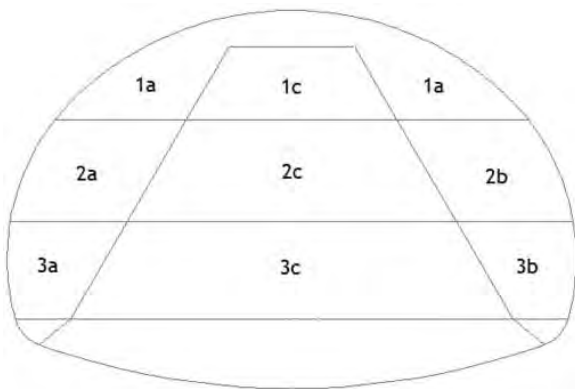
Fig.4 Construction procedures for the three-bench with reserved core soil

cement ratio of 1:1. The advanced small pipes are 5m long each and the external angle of the vault is between 10° and 15°. Then, cut and excavate core soils 1c, 2c and 3c within the range of 1m by the machine. After excavation of core soils, excavate the upper bench 1a by 1m and set up the preliminary supports, i.e. spray 4cm-thick shot concrete, rack the steel arch centering and place the steel legs. Upon the completion of bolting, keep spraying cement till it reaches the design thickness of 28cm. Next, excavate the side wall of the medium bench 2a 5m behind bench 1, spray 4cm of concrete, set up the initial steel arch centering of the medium bench, and place the steel legs. The side wall of the 2b bench should be excavated by a certain distance behind the side wall of 2a. The excavation of 3a and 3b should follow the same order as that of 2a and 2b.

On this basis, the authors edit the FLAC^{3D} roadway excavation program. Fig.5 displays the sectional view at the axle center of the roadway after excavation in the designed range.

3. Parameters for inversion and range determination

3.1 Sensitivity analysis

Based on Nishihara model, this study takes the degradation of surrounding rocks as the object of inversion
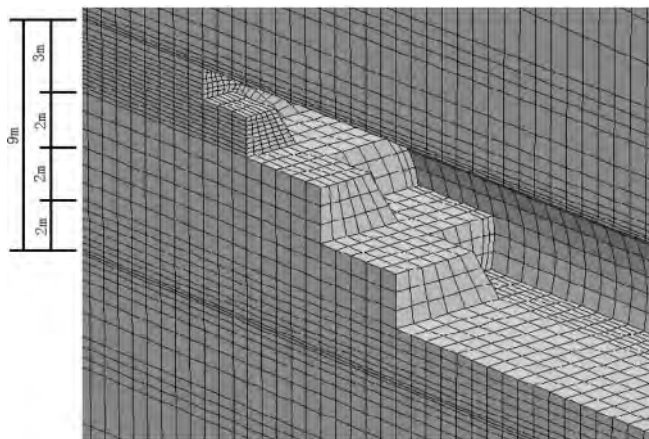

Fig.5 The sectional view at the axle center

and carries out inversion of 8 parameters. Theoretically, all parameters should be subjected to the inversion. However, the scale of solution will increase with the number of parameters for inversion, resulting in the "curse of dimensionality" [11, 12]. The parameters for inversion are normally selected by two principles: First, starting from the design intent, grasp the main contradiction and reduce the number of objects for inversion; second, select highly sensitive parameters for inversion [13]. In reference to the sensitivity analysis for system stability [14], this study analyzes the sensitivity of objective functions against the parameters for inversion, sieves out the parameters with huge impact on objective functions, and thus completes the selection of parameters for inversion. The values of parameters having less sensitivity are determined by experience.

The inversion is performed with surrounding rock elasticity modulus, cohesive strength, angle of friction, Kelvin shear modulus, Kelvin coefficient of viscosity and Maxwell shear modulus. The intermediate values of the spans for inversion parameters are collected into the benchmark parameter set. In the analysis of sensitivity of volume modulus b against vault subsidence u, for example, the parameters other than density are fixed to their baseline values. In this way, the authors obtain the relationship between the density (independent variable) and vault subsidence (dependent variable) as follows:

$$U = (b_1^*, b_2^*, ..., b_k^* b_{k+1}^*, ..., b_n^*) = \varphi_k(b_k) \qquad ... \quad (1)$$

According to the equation above, authors draw the system's characteristic curve $U - \varphi_k(b_k)$, which reflects the sensitivity of vault subsidence U against parameter d_k. Table 1 shows the numerical calculation results of the sensitivity analysis.

3.2 Uniform design based sample structure

The orthogonal design method is one of the most common and effective approaches for experimental design. It picks the representative points of orthogonality through comprehensive tests [15]. Six factors are taken into account, including surrounding rock elasticity modulus (bulk), cohesive strength (coh), angle of friction (fric), Kelvin shear modulus (E_K), Kelvin coefficient of viscosity (η_K) and Maxwell shear modulus (η_M). In the displacement inversion, uniform design table U21 (21^6) (Table 2) is employed to divide each parameter into 10 levels for 21 tests and for building the learning samples and test samples of the neural network.

4. Inversion of surrounding rock parameters with BP neural network
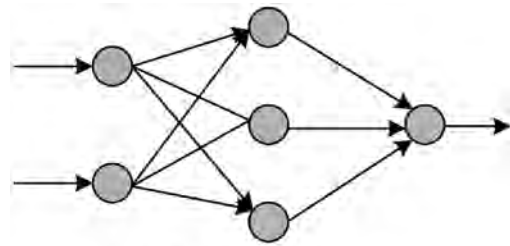
4.1 Features of BP neural network

Artificial neural network is a complex network system formed by entities and simple neurons connected with each
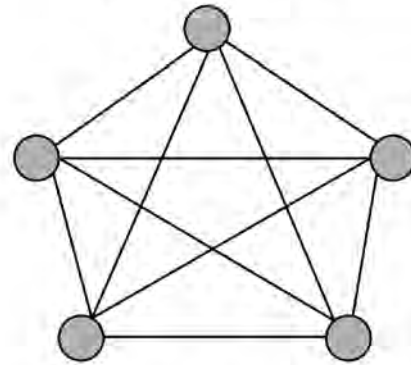
TABLE 1. SENSITIVITY ANALYSIS TABLE

Analysis object		Bulk/GPa	Coh/MPa	Ten/MPa	φ	EK/GPa.d	hK/GPa.d	EM/GPa	U30/mm
Bulk	max	0.815	0.25	0.25	27	4.5	10	3.25	6.32
	min	0.345	0.25	0.25	27	4.5	10	3.25	7.86
Coh	max	0.58	0.4	0.25	27	4.5	10	3.25	8.02
	min	0.58	0.1	0.25	27	4.5	10	3.25	6.04
Ten	max	0.58	0.25	0.4	27	4.5	10	3.25	7.24
	min	0.58	0.25	0.1	27	4.5	10	3.25	7.44
φ	max	0.58	0.25	0.25	32.5	4.5	10	3.25	7.96
	min	0.58	0.25	0.25	21.5	4.5	10	3.25	6.42
EK	max	0.58	0.25	0.25	27	8	10	3.25	4.82
	min	0.58	0.25	0.25	27	1	10	3.25	10.72
çK	max	0.58	0.25	0.25	27	4.5	15	3.25	4.8
	min	0.58	0.25	0.25	27	4.5	5	3.25	8.4
EM	max	0.58	0.25	0.25	27	4.5	10	6	6.02
	min	0.58	0.25	0.25	27	4.5	10	0.5	8.68

TABLE 2: U26 (21[6]) TABLE

	1	2	3	4	5	6
1	1	4	10	13	16	19
2	2	8	20	5	11	17
3	3	12	9	18	6	15
4	4	16	19	10	1	13
5	5	20	8	2	17	11
6	6	3	18	15	12	9
7	7	7	7	7	7	7
8	8	11	17	20	2	5
9	9	15	6	12	18	3
10	10	19	16	4	13	1
11	11	2	5	17	8	20
12	12	6	15	9	3	18
13	13	10	4	1	19	16
14	14	14	14	14	14	14
15	15	18	3	6	9	12
16	16	1	13	19	4	10
17	17	5	2	11	20	8
18	18	9	12	3	15	6
19	19	13	1	16	10	4
20	20	17	11	8	5	2
21	21	21	21	21	21	21

(a) Feedforward network

(b) Feedback network

Fig.6 Structural graph of neural network

other. It reflects many basic features of human brain, which is a highly complex non-linear dynamic system [16]. Single neurons with simple structure and functions are linked up to form a neural network with complex behaviours. From the perspective of the connection type of the network topology, the neural network can be categorized as the feedforward network and feedback network. (Fig.6) In the feedforward network, each neuron receives input from the previous layer and sends outputs to the next layer without feedback. In the feedback network, all nodes are the computing elements that receives inputs and forms an undirected graph with outputs [17]. BP neural network is a typical feedforward neural network.

BP neural network is a multi-layer feedforward neural network, in which signal inputs or outputs are transmitted layer by layer. The signals are processed by the input layer, transmitted to the hidden layer, and sent out from the output layer. The state of neurons of each layer only affects the state of neurons of the following layer. In error back propagation, if the output layer fails to get the expected output, it will switch to back propagation and adjust the network weight and threshold according to predicted errors so that the

predicted outputs of the network could approximate the expected output. The network topology of the BP neural network is shown in Fig.7.
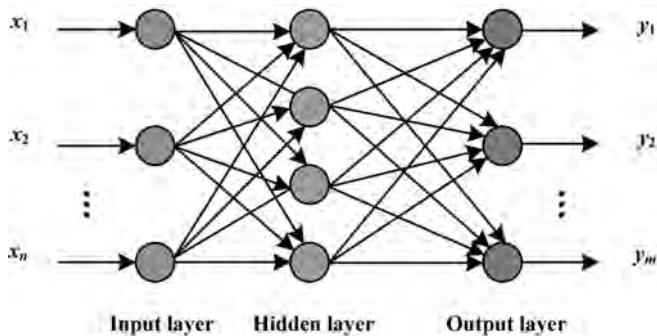

Fig.7 Topology of BP network

4.2 AUTHOR INFORMATION

In the inversion process, sample training, test and computation of the BP neural network are achieved with computer software. The MATLAB neural network toolbox provides BP network analysis and design with BP neural networks, BP algorithms, and improved BP algorithms with multiple functions. It can be conveniently and intuitively applied in the BP neural network.

(1) Normalization

Owing to the wide span of input and output vectors, it is necessary to normalize such vectors and translate them into data within the range [0, 1] for the purpose of improving the training effect in the function training. Normalization should be carried out by the following equation: Full names of authors are preferred in the author field, but are not required.

$$\hat{x}_i = \frac{x_i - x_{\min}}{x_{\max} - x_{\min}} \qquad ... \quad (2)$$

where x_i is the ith input of the network, x_{min} is the minimum input and x_{max} is the maximum input.

In addition, counter-normalization is made to the network output:

$$\bar{y}_i = \bar{x}_i(x_{\max} - x_{\min}) + x_{\min} \qquad ... \quad (3)$$

where y_i is the ith network output, y_{min} is the minimum output and y_{max} is the maximum output.

(2) Establishment of BP neural network

The feedforward back propagation (BP network) is created with MATLAB in the following manner [18]:

net = newff (PR, [S$_1$ S$_2$...SN$_1$], {TF$_1$ TF$_2$ ...TFN$_1$}, BTF, BLF, PF)

Where net = newff: create the feedforward back propagation network in the form of dialog box;

PR: the R×2 dimension matrix formed with maximum and minimum values of input in each group (there are in total R groups of input elements);

Si: the length of the ith layer (there are in total NI layers);

TFI: the transmission function, which can be set to "tansig" (default), "logsig" or "purelin".

BTF: network training function, which can be set to "trainlm" (default), "trainbfg", "trainrp" or "graingd".

BLF: BP learning function of weight and threshold, which can be set to "learngd" or "learngdm" (default).

PF: network error performance function, which can be set to "mse" (default) or "msereg".

(3) Design of the neural network structure

In 1989, Robert Hecht-Nielson proved that any continuous function in any closed interval could be approached with a BP network with the hidden layer. Therefore, a 3-layer BP network is capable of mapping any n-th dimension to the m-th dimension. In this paper, a BP neural network with a hidden layer is adopted.

Another important issue is the number of nodes of the hidden layer. However, there is still no unified and comprehensive theories regarding the issue. If there are too few nodes in the hidden layer, the network will have low accuracy due to the difficulty in learning and the want of training. On the contrary, if there are too many nodes, the network will face inconsistent fitting and poor generalization because of the increase of training practice and lengthy learning time [19].

Hence, the number of nodes in the hidden layer is determined by the following equations.

$$n_1 = 2n + 1 \qquad ... \quad (4)$$

$$n_1 = \sqrt{n + m} + c \qquad ... \quad (5)$$

$$n_1 \geq \log_2 n \qquad ... \quad (6)$$

where n_1 is the number of nodes in the hidden layer; n is the number of nodes of the input layer; m is the number of nodes of the output layer; c is a constant ranging from 1 to 10.

In this model, n = 9 and m = 6.

According to the above equations, the number of the nodes of the hidden layer is as follows:

$$n_1 = 19 \qquad ... \quad (7)$$

$$n_1 = \sqrt{n + m} + c = 5 \sim 20 \qquad ... \quad (8)$$

$$n_1 \geq 2 \qquad ... \quad (9)$$

To sum up, the number of nodes in the hidden layer falls in the range of 4~20. Thus, the number of hidden layers are set in the range of 4~20 with the goal of minimizing the total error of the system. The cycles are built according to the number of hidden layers. Besides, the number of the hidden

	Bulk /GPa	Coh /MPa	fric /°	EK /GPa	ηK /GPa .day	EM /GPa	D2 /mm	D4 /mm	D6 /mm	D8 /mm	D10 /mm	D12 /mm
1	0.345	0.145	26.5	5.2	12.5	5.45	0.4196	0.8952	1.4112	1.9632	2.4872	2.9712
2	0.369	0.205	32	2.4	10	4.9	0.4222	0.9178	1.4718	2.0798	2.7298	3.3818
3	0.392	0.265	25.9	6.95	7.5	4.35	0.3562	0.798	1.3266	1.9166	2.4946	3.0106
4	0.416	0.325	31.4	4.15	5	3.8	0.4526	1.0252	1.7152	2.4832	3.2712	4.0172
5	0.439	0.385	25.4	1.35	13	3.25	0.3776	0.8428	1.3714	1.9656	2.6136	3.2616
6	0.463	0.13	30.9	5.9	10.5	2.7	0.3262	0.7034	1.176	1.714	2.278	2.79
7	0.486	0.19	24.8	3.1	8	2.15	0.3144	0.6632	1.0654	1.5314	2.0014	2.5254
8	0.533	0.31	24.3	4.85	13.5	1.05	0.2006	0.4424	0.761	1.1494	1.6384	2.2324
9	0.557	0.37	29.8	2.05	11	0.5	0.1428	0.4166	0.829	1.328	1.93	2.708
10	0.58	0.115	23.7	6.6	8.5	5.73	0.3744	0.8094	1.3064	1.8124	2.3004	2.7564
11	0.604	0.175	29.2	3.8	6	5.18	0.4626	1.0008	1.6018	2.2498	2.9038	3.5018
12	0.627	0.235	23.2	1	14	4.63	0.3466	0.7724	1.2488	1.767	2.301	2.841
13	0.651	0.295	28.7	5.55	11.5	4.08	0.3536	0.8166	1.3306	1.8886	2.4466	2.9666
14	0.674	0.355	22.6	2.75	9	3.53	0.418	0.9322	1.5322	2.2042	2.8962	3.5922
15	0.698	0.1	28.1	7.3	6.5	2.98	0.263	0.5692	0.9086	1.2906	1.6766	2.0266
16	0.721	0.16	22.1	4.5	14.5	2.43	0.2786	0.6408	1.0756	1.6076	2.2036	2.7776
17	0.745	0.22	27.6	1.7	12	1.88	0.4016	0.8878	1.4418	2.0858	2.7758	3.4858
18	0.768	0.28	21.5	6.25	9.5	1.33	0.2902	0.6244	1.0174	1.4574	1.9314	2.4614
19	0.792	0.34	27	3.45	7	0.775	0.2034	0.5058	0.878	1.344	1.91	2.566
20	0.815	0.4	32.5	8	15	6	0.3616	0.8134	1.287	1.745	2.171	2.513

TABLE 4: NETWORK TEST SAMPLES

	Bulk /GPa	Coh /MPa	fric /°	EK /GPa	ηK /GPa	EM /GPa	D2 /mm .day	D4 /mm	D6 /mm	D8 /mm	D10 /mm	D12 /mm
1	0.51	0.25	30.3	7.65	5.5	1.6	0.305	0.7268	1.1908	1.7728	2.4558	3.2148

layers at the minimum total error of the system is taken as the number of nodes of the hidden layer for network training. Through comparison, it is revealed that the total error of the system was minimum when the number of nodes of the hidden layer is $n_1 = 15$.

During network training, the rationality of the value selection of learning rate has a direct impact to the learning speed, convergence performance and promotion capability. If the learning rate is too slow, the training time will be greatly lengthened and the convergence rate will be slowed down. In contrast, if the learning rate is too fast, the error function value will remain on a high level, leading to non-convergence of algorithms. To ensure computational stability, the learning rate of fixed learning rate algorithms should be as slow as possible within the permission of the computation time. In this paper, the learning rate is set as 0.01.

4.3 NETWORK TRAINING AND INVERSION OF RHEOLOGICAL PARAMETERS OF THE SURROUNDING ROCKS

FLAC^{3D} finite element software is adopted for numerical simulation of parameters at different levels to obtain vault

subsidence displacement of D2, D4, D6, D8, D10 and D12 with different combinations of the parameters. In total, 20 parametric combinations are selected as input samples for neural network training. The corresponding calculated vault subsidence displacements are taken as the output samples of network training (Table 3). The rest 1 parametric combination and its calculated vault subsidence displacement are taken as the sample for testing the performance of the training network (Table 4).

There are 9 neurons on the input layer and 6 on the output layer. According to the general design principles, the input layer and the hidden layer are built with the hyperbolic tangent activation function tansig; the activation function between the hidden layer and the output layer is purelin; the training function is trainbfg and the expected error is 0.01. In Table 3, Columns 7-15 show the displacement data of the parametric combinations and the displacement values generated by FLAC^{3D}; Columns 1-6 display the parametric combinations for inversion, which are imported to the BP neural network as training samples. Fig.8 records the errors during the training of samples.

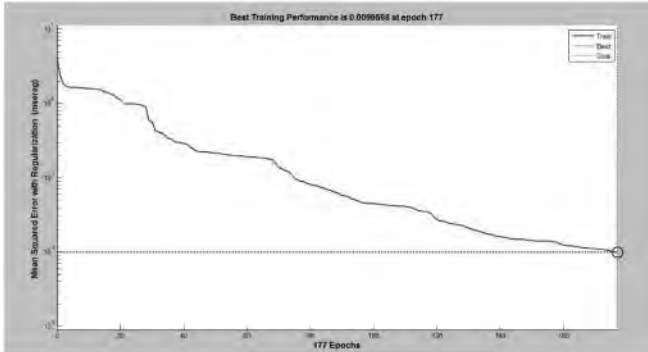| Output parameters	Bulk/GPa	Coh/MPa	fric/°	EK/GPa	ηK/GPa	EM/GPa.day
	0.534	0.236	31.5	7.51	5.318	1.55

Fig.8 Error records in the network training process

TABLE 6: ACTUALLY MEASURED LOCATION OF THE VAULT SUBSIDENCE

Time	D2	D4	D6	D8	D10	D12
Vault subsidence (mm)	0.4	0.8	1.4	1.6	2.2	2.4

TABLE 7: PARAMETER VALUES OBTAINED FROM INVERSION

Parameters	Bulk/GPa	Coh/MPa	fric/°	EK/GPa	ηK/GPa	EM/GPa.day
	0.738	0.27	27.48	2.7	8.91	1.802

The displacement data in Columns 7-5 in Table 3 are imported to the network for simulation. The results are as follows:

The simulation results are compared to the network test samples in Columns 1-6. The mean error is 4.26%, which basically meets the engineering requirements.

After network training, the actually measured data in Table 6 are imported into the network for displacement inversion. The resulting parameters of surrounding rocks are shown in Table 7.

The above tests demonstrate that the BP neural network can resolve the problems of long observation period and unrepeatability if it is applied in inversion of the rheological parameters of surrounding rocks.

5. Conclusions

For the purpose of resolving the difficulties in undermining the rheological parameters resulted from testing conditions and external environment, this paper conducts inversion of the rheological parameters of surrounding rocks based on the BP neural network. Taking a mine roadway as an example, the authors rely on BP neural network to determine rheological parameters of the roadway. In consideration of the vault subsidence data in the entrance section, authors apply FLAC^{3D} in numerical simulation, adopts BP neural network for network learning and sample training, and performs displacement inversion of the rheological parameters of the surrounding rocks in the section. It is proved by tests that the back analysis is feasible and applicable in the determination of the rheological parameters of the surrounding rocks.

References

1. Griggs, D. (1939): "Creep of rocks," *Journal of Geol*, vol. 47, no. 3, pp. 225-251, Apr. 1939.

2. Chen, Z. J., Kang, W. F. and Huang, J. P. (1991): "Rock Enclosed Stress, Creep and Capacity Expansion and Constitutive Equation," *Rock Mechanics and Engineering*, vol. 10, no. 4, pp. 299-312, Dec. 1991.

3. Shi, Y. C. and Zhang, Z. Y. (1991): "Study on Rheological Property of Uralitization Basalt Weak Rock Belt on Right Dam Abutment of Ertan Hydropower Station," *Journal of Chengdu College of Geology*, no. 2, pp. 72-81, Feb. 1991.

4. Zhou, H. M. and Xu, P. (2007): "Study on Rock Mass Compression Creep Test of Side Slope of Three-gorge Permanent Navigation Lock," *Rock Mechanics and Engineering*. pp. 1882-1885, 2007.

5. Gazzaz, N. M., Yusoff, M. K., Ramli, M. F., Juahir, H. and Aris, A. Z. (2015): "Artificial neural network modeling of the water quality index using land use areas as predictors," *Water Environment Research A Research*, vol. 87, no. 2, pp. 99-112, Feb. 2015.

6. Giri, A. and Singh, N. B. (2014): "Comparison of Artiûcial Neural Network Algorithm for Water Quality Prediction of River Ganga," *Environmental Research Journal*, vol. 8, no. 2, pp. 55-63, 2014.

7. Khairi, M. T. M., Ibrahim, S., Yunus, M. A. M., Faramarzi, M. and Yusuf, Z. (2016): "Artificial Neural Network Approach for Predicting the Water Turbidity Level Using Optical Tomography," *Arabian Journal for Science and Engineering*, vol. 41, no. 9, pp. 1-11, Sep. 2016. DOI: 10.1007/s13369-015-1904-6.

8. Han, H. G. and Qiao, J. F. (2014): "Nonlinear model-predictive control for industrial processes: an application to wastewater treatment process," *IEEE Transactions on Industrial Electronics*, vol. 61, no. 4, pp. 1970-1982, Apr. 2014. DOI: 10.1109/TIE.2013.2266086